

## ORIGINAL ARTICLE

Comparison of velocity- and acceleration-selective arterial spin labeling with [<sup>15</sup>O]H<sub>2</sub>O positron emission tomographySophie Schmid<sup>1,4</sup>, Dennis FR Heijtel<sup>2,4</sup>, Henri JMM Mutsaerts<sup>2</sup>, Ronald Boellaard<sup>3</sup>, Adriaan A Lammertsma<sup>3</sup>, Aart J Nederveen<sup>2</sup> and Matthias JP van Osch<sup>1</sup>

In the last decade spatially nonselective arterial spin labeling (SNS-ASL) methods such as velocity-selective ASL (VS-ASL) and acceleration-selective ASL have been introduced, which label spins based on their flow velocity or acceleration rather than spatial localization. Since labeling also occurs within the imaging plane, these methods suffer less from transit delay effects than traditional ASL methods. However, there is a need for validation of these techniques. In this study, a comparison was made between these SNS-ASL techniques with [<sup>15</sup>O]H<sub>2</sub>O positron emission tomography (PET), which is regarded as gold standard to measure quantitatively cerebral blood flow (CBF) in humans. In addition, the question of whether these techniques suffered from sensitivity to arterial cerebral blood volume (aCBV), as opposed to producing pure CBF contrast, was investigated. The results show high voxelwise intracranial correlation (0.72 to 0.89) between the spatial distribution of the perfusion signal from the SNS-ASL methods and the PET CBF maps. A similar gray matter (GM) CBF was measured by dual VS-ASL compared with PET (46.7 ± 4.1 versus 47.1 ± 6.5 mL/100 g/min, respectively). Finally, only minor contribution of aCBV patterns in GM to all SNS-ASL methods was found compared with pseudo-continuous ASL. In conclusion, VS-ASL provides a similar quantitative CBF, and all SNS-ASL methods provide qualitatively similar CBF maps as [<sup>15</sup>O]H<sub>2</sub>O PET.

*Journal of Cerebral Blood Flow & Metabolism* (2015) **35**, 1296–1303; doi:10.1038/jcbfm.2015.42; published online 18 March 2015

**Keywords:** [<sup>15</sup>O]H<sub>2</sub>O positron emission tomography; acceleration-selective arterial spin labeling; perfusion imaging; velocity-selective arterial spin labeling

## INTRODUCTION

Arterial spin labeling (ASL) is a magnetic resonance (MR) technique that uses arterial blood as an endogenous tracer for noninvasive and quantitative local tissue perfusion measurements.<sup>1</sup> Conventional ASL methods label blood magnetically by inversion or saturation in a slab proximal to the imaging region. Subsequently, the label image is acquired after a postlabeling delay (PLD), which is chosen approximately equal to the longitudinal relaxation time of blood (T<sub>1</sub>) for cerebral perfusion imaging. The PLD represents a compromise between loss of label because of T<sub>1</sub> decay and transport time for labeled blood to reach the microvascular bed.<sup>2</sup> A so-called control image is obtained by repeating the sequence without labeling blood. By subtracting the label image from the control image, contributions from static tissue will be removed. Therefore, solely magnetization of inflowing tagged spins will be measured, resulting in a perfusion-weighted image. To gain sufficient signal-to-noise ratio (SNR) multiple interleaved repetitions of both label and control sequences are performed.

Currently, pseudo-continuous ASL (pCASL) is considered to be the most reliable and robust ASL technique.<sup>3</sup> However, when arrival of the labeled blood in the tissue is delayed—for example, because of pathophysiological conditions—a longer PLD is required, leading to more relaxation of the label and thereby

lower SNR. However, when the PLD is chosen too short, a severe underestimation of the cerebral blood flow (CBF) will occur. Selecting a proper PLD for accurate CBF values in clinical pathologies represents a delicate balance and would frequently lead to a need for too many signal averages to be clinically practical.

Recently, a new family of ASL techniques has been introduced. These spatially nonselective ASL (SNS-ASL) methods label spins based on their flow velocity (velocity-selective ASL, VS-ASL) or acceleration (acceleration-selective ASL, AccASL) rather than spatial localization.<sup>4–7</sup> As the label is generated globally, i.e., also within the imaging plane, it is labeled much closer to the capillaries. Therefore, the time to reach the tissue, the so-called transit delay, is smaller and more uniform and consequently these SNS-ASL techniques have the potential to be used even under slow and collateral flow conditions.<sup>8,9</sup> Although all these SNS-ASL methods are regarded to reflect perfusion information, one of them is thought to be purely CBF weighted (dual VS-ASL), while the others are thought to be weighted to mixed haemodynamic parameters, both CBF and CBV (single VS-ASL and AccASL).

Clearly, there is a need for validation of this new family of ASL techniques. Dual VS-ASL has already been compared with traditional ASL techniques,<sup>6,10</sup> and xenon computed tomography (CT),<sup>8</sup> but single VS-ASL and AccASL have only been compared

<sup>1</sup>Department of Radiology, C. J. Gorter Center for High Field MRI, Leiden University Medical Center (LUMC), Leiden, The Netherlands; <sup>2</sup>Department of Radiology, Academic Medical Center, Amsterdam, The Netherlands and <sup>3</sup>Department of Radiology & Nuclear Medicine, VU University Medical Center, Amsterdam, The Netherlands. Correspondence: S Schmid, MSc, Department of Radiology, C. J. Gorter Center for High Field MRI, Leiden University Medical Center (LUMC), C3-Q, Albinusdreef 2, Leiden 2333 ZA, The Netherlands. E-mail: s.schmid@lumc.nl

This research was supported by the Dutch Technology Foundation STW, applied science division of NWO and the Technology Program of the Ministry of Economic Affairs and by grants 0903-044 and 1002-031 from the Nuts-Ohra Foundation (Amsterdam, The Netherlands).

<sup>4</sup>These authors contributed equally to this work.

Received 1 September 2014; revised 10 February 2015; accepted 16 February 2015; published online 18 March 2015

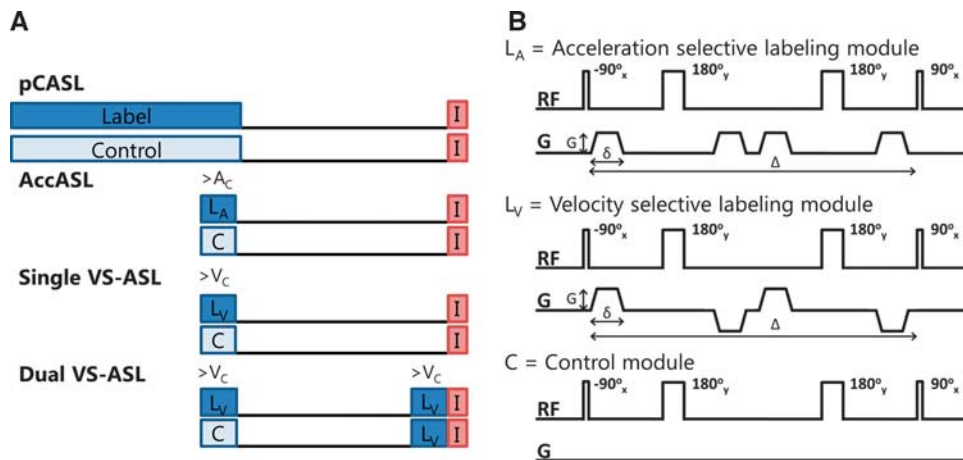


**Figure 1.** (A) Schematic pulse sequence diagrams of the different arterial spin labeling methods, where  $L_A$  is the acceleration-selective labeling module,  $L_V$  is the velocity-selective labeling module, and C is the control module and I is imaging. (B) Schematic depiction of the radio frequency (RF) pulses and gradients (G) in the labeling modules of acceleration-selective arterial spin labeling (AccASL), velocity-selective ASL (VS-ASL), and in the control (C) condition. pCASL, pseudo-continuous ASL.

with pCASL.<sup>7</sup> None of these SNS-ASL techniques have, however, been compared with the gold standard for quantifying CBF in humans: [<sup>15</sup>O]H<sub>2</sub>O positron emission tomography (PET).<sup>11</sup> Besides providing parametric CBF images, [<sup>15</sup>O]H<sub>2</sub>O PET can also be used to generate arterial cerebral blood volume (aCBV) images.

Therefore, the primary aim of this study was to compare dual VS-ASL with [<sup>15</sup>O]H<sub>2</sub>O PET-derived CBF in a quantitative way. As secondary aim, the qualitative correspondence of dual VS-ASL as well as of single VS-ASL and AccASL with PET was studied. Finally, it will be investigated whether these SNS-ASL methods have a stronger correlation to aCBV signal distribution compared with the traditional ASL method, again using [<sup>15</sup>O]H<sub>2</sub>O PET as a standard.

## MATERIALS AND METHODS

### Subjects and Study Protocol

This study was performed in compliance with regulations of the local institutional review boards of the participating centers and federal authorities according to the Declaration of Helsinki 'Ethical Principles for Medical Research Involving Human Subjects' and in accordance with the guidelines for Good Clinical Practice (CPMP/ICH/135/95) and written informed consent was obtained from each participant before inclusion. This study was part of another study, where the accuracy and precision of pCASL measurements were compared head-to-head with [<sup>15</sup>O]H<sub>2</sub>O PET, by means of a test–retest paradigm as described by Heijtel *et al.*<sup>12</sup> In addition to the previously described results, we studied three different SNS-ASL scans in the current study, which were performed during the second visit. Only the healthy subjects who completed all required scans (three SNS-ASL scans, a pCASL scan, a pCASL scan with vascular crushing as well as the [<sup>15</sup>O]H<sub>2</sub>O PET scan) were included in the present study ( $n = 13$ , 7 male and 6 female; age 20 to 24 years).

All MR scans were performed on a Philips 3T Intera system (Philips Healthcare, Best, the Netherlands) using an eight-channel sensitivity encoding (SENSE) head coil at the Academic Medical Center in Amsterdam. All PET examinations were performed on a Philips Gemini TF-64 PET/CT system (Philips Healthcare, Cleveland, TN, USA) at the VU University Medical Center in Amsterdam. The PET and MR scans were performed in a random order with a maximum of 7 days between both sessions.

Three types of SNS-ASL approaches were compared with [<sup>15</sup>O]H<sub>2</sub>O PET and schematic pulse sequence diagrams of these ASL methods are shown in Figure 1A. The first type, which will be referred to as 'single VS-ASL', uses one velocity-selective labeling module and labels all spins that flow faster than a predefined cutoff velocity ( $V_c$ ). This is irrespective of whether these spins are located in arterial or venous blood and therefore this sequence is thought to have some CBV weighting. The second type, which will be referred to as 'dual VS-ASL', is similar to single VS-ASL, except that a second

velocity-selective labeling module is added just before imaging in both the label and control conditions. This suppresses all spins accelerating in the PLD between the labeling modules, which is assumed to be the venous component.<sup>5</sup> This is the only quantitative SNS-ASL method and is proposed to be predominantly CBF weighted.<sup>6</sup> In the literature, this technique is referred to as VS-ASL, but to provide more insight into the labeling process, single VS-ASL was also included into this study, thereby requiring a clear distinguished terminology. The most recently introduced and third type is AccASL, which contains only a single labeling module and labels all spins that accelerate or decelerate during the labeling module above a certain cutoff acceleration ( $A_c$ ) (or deceleration). It has been suggested that the signal is of mixed haemodynamic origin; including both CBF and CBV weighting. The only difference between the velocity-sensitive and acceleration-sensitive labeling modules is the sign of the second and fourth gradients in the labeling module, as shown in Figure 1B, inducing an effective zero first-gradient moment, giving no velocity sensitization, but acceleration sensitization because of a second-gradient moment.<sup>7,13</sup>

pCASL, as used in the present study for reference purposes, was previously compared with [<sup>15</sup>O]H<sub>2</sub>O PET showing good resemblance.<sup>12,14</sup>

### Magnetic Resonance Imaging Acquisition

Single VS-ASL, dual VS-ASL, and AccASL were acquired with interleaved label and control images. The labeling module parameters for VS-ASL, which determine the velocity sensitivity, were 22 mT/m for the amplitude of the gradients (G), 1 ms for the gradient duration ( $\delta$ ) and 30 ms for the time between the 90° radio frequency (RF) pulses ( $\Delta$ ), corresponding to a cutoff velocity ( $V_c$ ) of 2 cm/s. The labeling module parameters for AccASL, which determine the acceleration sensitivity, were  $G = 30$  mT/m,  $\delta = 1$  ms, and  $\Delta = 30$  ms, corresponding to a cutoff acceleration ( $A_c$ ) of 2.3 m/s<sup>2</sup>. A schematic depiction of these labeling modules is shown in Figure 1B. Velocity and acceleration encodings were only applied along the slice encoding direction (approximately feet-head direction). During the postlabeling delay of 1,600 ms for all three techniques background suppression was applied using two adiabatic nonselective inversion pulses at 50 and 1,150 ms after labeling to increase the contrast-to-noise ratios.<sup>15–17</sup> The postacquisition delay, the time between the postacquisition nonselective saturation and subsequent labeling module, was set to 2,000 ms. An overview of all imaging parameters can be found in Table 1.

Balanced pCASL was used as a reference representing spatially selective or 'conventional' ASL methods.<sup>18</sup> The labeling duration was 1,650 ms with a pulse duration of 0.5 ms, a 0.5 ms pause between the pulses, and an 18° flip angle combined with a 0.6 mT/m average gradient in the direction of the blood flow. Pseudo-continuous ASL scans were acquired with and without vascular crushing ( $V_c = 5$  cm/s) to study the effect of macrovascular crushing. For positioning of the pCASL labeling plane, a time-of-flight angiogram was acquired. The location of labeling slab was positioned such that it was perpendicular to the main brain-feeding arteries and intercepts with the v3 segment of the vertebral arteries.<sup>19</sup>

**Table 1.** Scanning parameters, the various scans in the MRI protocol

Method	ASL perfusion					Anatomical	$M_{0,CSF}$	Labeling efficiency	$T_{1,a}$
	Spatially nonselective ASL			Conventional ASL					
	Single VS-ASL	Dual VS-ASL	AccASL	pCASL	pCASL crush				
FOV (mm <sup>2</sup> )	240 × 240	240 × 240	240 × 240	240 × 240	240 × 240	240 × 240	240 × 240	230 × 230	230 × 230
Resolution (mm <sup>2</sup> )	3 × 3	3 × 3	3 × 3	3 × 3	3 × 3	1 × 1	3 × 3	0.45 × 0.45	1.5 × 1.5
Slice thickness (mm)	7	7	7	7	7	1	7	4	2
Slices	17	17	17	17	17	200	17	1	1
TR/TE (ms)	4,248/14	4,248/14	4,248/14	3,850/14	3,921/17	7.0/3.1	2,825–4,625/14	15/5.1	10,000/10.9
Read-out	GE–SSh–EPI	GE–SSh–EPI	GE–SSh–EPI	GE–SSh–EPI	GE–SSh–EPI	3D–FFE	GE–SSh–EPI	2D–FFE	SSh–EPI
Labeling duration or $\Delta$ (ms)	30	30	30	1,650	1,650	—	—	—	—
PLD (ms)	1,600	1,600	1,600	1,525	1,525	—	1,100	—	190
$\Delta$ TI (ms) /nTI	—	—	—	—	—	—	200/10	—	150/60
Bsup (ms)	50/1,150	50/1,150	50/1,150	1,680/2,860	1,680/2,860	—	—	—	—
G (mT/m)	22	22	30	—	—	—	—	—	—
$\delta$ (ms)	1	1	1	—	—	—	—	—	—
$V_C$ or $A_C$	2 cm/s	2 cm/s	2.3 m/s <sup>2</sup>	—	5 cm/s	—	—	80 cm/s	—
SENSE	2.5	2.5	2.5	2.5	2.5	—	2.5	—	3
Fat suppression	SPIR	SPIR	SPIR	SPIR	SPIR	—	SPIR	—	—
NSA	35	35	35	54	38	1	2	2	6
$T_{acq}$ (seconds)	297	297	297	419	301	245	78	61	130

Abbreviations: 2D, two dimensional; 3D, three dimensional;  $\delta$ , gradient duration of the labeling module;  $\Delta$ , time between the 90° RF pulses of the labeling module;  $A_C$ , cutoff acceleration; AccASL, acceleration-selective arterial spin labeling; Bsup, background suppression pulses; CSF, cerebrospinal fluid; EPI, echo planar imaging; FFE, fast field echo; FOV, field of view; G, amplitude of the gradients in the labeling module; GE, gradient echo; IR, inversion recovery; MRI, magnetic resonance imaging; NSA, number of signal averages; PC-MRI, phase-contrast MRI; pCASL, pseudo-continuous ASL; PLD, postlabeling delay; SENSE, sensitivity encoding; MPRAGE, magnetization prepared rapid acquisition gradient echo; Multi-TI IR, multi inversion time inversion recovery; RF, radio frequency; SPIR, spectral presaturation inversion recovery; SSh, single shot;  $T_{acq}$ , acquisition time; TE, echo time; TI, inversion time; TR, repetition time;  $V_C$ , cutoff velocity; VS-ASL, velocity-selective ASL. <sup>a</sup>Multi-TI IR scan was implemented as a control-only pCASL scan with ‘labeling duration’ of 650 ms.

For ASL quantification purposes, an inversion recovery sequence with equal readout properties as the ASL sequence was acquired with 10 different inversion times to estimate the longitudinal magnetization ( $M_0$ ), followed by a  $T_1$ -mapping sequence of the venous blood to estimate the longitudinal relaxation of arterial blood ( $T_{1a}$ ).<sup>20</sup> In addition, to estimate the pCASL labeling efficiency a phase-contrast MRI was performed immediately after the pCASL scans, using a slice positioned at the center of the pCASL labeling plane, to measure the blood flow velocity in the brain-feeding arteries.

For anatomic reference a whole brain  $T_1$ -weighted magnetization prepared rapid acquisition gradient echo (MPRAGE) image was acquired with a 1-mm isotropic voxel size.

### Magnetic Resonance Imaging Postprocessing

The Oxford Centre for Functional MRI of the Brain (FMRIB)’s Software Library (FSL, Oxford, UK) was used for realigning the unsubtracted ASL images<sup>21,22</sup> and the time series were motion corrected with motion correction FMRIB’s linear image registration tool (MCFLIRT, FSL, Oxford, UK) with a six-parameter rigid transformation.<sup>23</sup> Arterial spin labeling maps were obtained by pairwise subtracting the label from the control images and averaging over time. To enable a valid comparison of the temporal SNRs (tSNRs) between all different ASL methods, a fixed total ASL sequence duration of 5 minutes was chosen. To this end, 35 averages of the SNS-ASL scans and the first 38 averages of the pCASL scans were included in the calculation of the tSNR, using the mean and s.e.m.

Subsequently, CBF was calculated for dual VS-ASL according to the following equation:<sup>10</sup>

$$CBF_{VS-ASL} = \frac{\Delta M \cdot e^{PLD/T_{1a}} \cdot e^{TE/T_{2a}}}{\rho \cdot M_{0a} \cdot \alpha_{VS-ASL} \cdot PLD \cdot \alpha_{BSup} \cdot (1 - e^{(PLD-TR)/T_{1a}})} \quad (1)$$

where CBF is the flow in mL/100 g/min,  $\Delta M$  the ASL signal intensity, PLD the postlabeling delay (1,600 ms for the first slice and increases with 35 ms for each after slice to correct for the ascending slice time delay),  $T_{1a}$  the longitudinal relaxation of arterial blood (as estimated by  $T_1$  mapping of venous blood in the sagittal sinus<sup>20</sup>),  $T_{2a}^*$  the  $T_2^*$  of arterial blood (50 ms<sup>24</sup>), TE the echo time (14 ms),  $\rho$  the density of brain tissue (1.05 g/mL<sup>25</sup>),  $M_{0a}$

the equilibrium magnetization of arterial blood as determined by a multiple time point inversion recovery scan (by fitting the  $M_0$  of cerebrospinal fluid (CSF) and multiplying the calculated value with the blood-water partition coefficient (0.76 mL water/mL blood<sup>25</sup>)),  $\alpha_{VS-ASL}$  the labeling efficiency (0.84<sup>9</sup>) derived from the duration of the labeling module (30 ms) and arterial  $T_2$  (170 ms<sup>26</sup>), and  $\alpha_{BSup}$  the decrease in labeling efficiency because of background suppression pulses (0.83<sup>16</sup>).

Cerebral blood flow was derived from the pCASL scans according to the following equation:<sup>12</sup>

$$CBF_{pCASL} = \frac{\Delta M \cdot e^{t_i/T_{1a}} \cdot e^{TE/T_{2a}}}{\rho \cdot M_{0a} \cdot 2\alpha_{pCASL} \cdot T_{1T} \cdot \alpha_{BSup} \cdot [e^{(t_i-PLD)/T_{1T}} - e^{(t_i-\tau-PLD)/T_{1T}}]} \quad (2)$$

with  $t_i$  being the tissue transit time (1,900 ms<sup>27</sup>),  $T_{1T}$  the longitudinal relaxation of brain tissue (1,200 ms for gray matter (GM)<sup>28</sup>),  $\alpha_{pCASL}$  the labeling efficiency derived from the phase-contrast MRI measurement (as simulated by Bloch equations based on the velocities in the labeled arteries<sup>29,30</sup>), PLD the postlabeling delay (1,525 ms for the first slice and increases with 35 ms for each after slice), and  $\delta$  and  $\tau$  the labeling duration (1,650 ms).

For the vascular-crushed pCASL scans it was assumed that only the ASL signal in relatively large arteries with a blood velocity > 5 cm/s was affected by crushing.<sup>31</sup> Therefore, quantification of these scans was performed using the same model as the noncrushed pCASL scans.

An in-plane 5-mm full width at half maximum Gaussian kernel was used to smooth all CBF images to obtain an image resolution comparable with that of [<sup>15</sup>O]H<sub>2</sub>O PET images and to have a similar smoothing process.

### Positron Emission Tomography Acquisition

Prior to scanning, all subjects received an indwelling radial artery cannula for blood sampling and a venous cannula in the opposite arm for administration of [<sup>15</sup>O]H<sub>2</sub>O. Each subject was positioned with the head in the center of the field of view and immobilized with a foam mold to minimize motion. First, a 1-minute low-dose CT transmission scan was acquired to enable correction of the subsequent emission scan for photon attenuation and scatter. Next, a dynamic emission scan was performed in three-dimensional acquisition mode, starting at the time of administration

of an intravenous bolus of 800 MBq [<sup>15</sup>O]H<sub>2</sub>O. This scan consisted of 25 frames with progressively increasing duration over a total scanning period of 10 minutes. The concentration in arterial blood was monitored continuously using an online blood sampler,<sup>32</sup> which was calibrated using three manual arterial blood samples, taken at 5.5, 8, and 10 minutes after injection.

### Positron Emission Tomography Postprocessing

The [<sup>15</sup>O]H<sub>2</sub>O PET data were reconstructed using the row-action maximum-likelihood algorithm brain reconstruction protocol as provided by the vendor (128 × 128 matrix, 2-mm isotropic voxel size), including all common corrections (random events, dead time, photon decay, attenuation, and scatter) required for quantification. Reconstructed images were smoothed with an isotropic 5-mm full width at half maximum Gaussian kernel, resulting in an image resolution of ~6.5 mm isotropic full width at half maximum. A single tissue compartment model with arterial blood volume fraction correction was used for CBF quantification:

$$C_T(t) = V_a \cdot C_a + (1 - V_a) \cdot f_{PET} \cdot e^{(-f_{PET} \cdot t \cdot V_T^{-1})} \otimes C_a(t) \quad [3]$$

where  $C_T$  is the tissue concentration of <sup>15</sup>O H<sub>2</sub>O,  $V_a$  the arterial blood volume (aCBV),  $C_a$  the arterial concentration of [<sup>15</sup>O]H<sub>2</sub>O,  $f_{PET}$  the blood

flow (CBF),  $t$  the time, and  $V_T$  the volume of distribution of the water. Subsequently, parametric CBF and aCBV images were generated from the smoothed dynamic images using a basis function method implementation of the single tissue compartment model with corrections for dispersion, delay, and arterial blood volume.<sup>33,34</sup>

### General Postprocessing

In FSL, the FMRIB's automated segmentation tool (FAST, FSL, Oxford, UK) was used to segment the anatomic T<sub>1</sub>-weighted scan of each subject into different tissue types (GM, white matter (WM), and CSF probability maps). All ASL and PET CBF maps were individually coregistered to the segmented GM probability map using FMRIB's linear image registration tool (FLIRT, FSL, Oxford, UK). A GM mask was generated using a threshold of 55% GM probability. The T<sub>1</sub>-weighted scan of each subject was registered to the Montreal Neurological Institute (MNI) template with FMRIB's nonlinear image registration tool (FNIRT, FSL, Oxford, UK). Subsequently, all coregistered perfusion images and GM masks were warped into MNI space using the same transformation parameters.

### Data Analysis

For each subject, the mean GM CBF was calculated for the dual VS-ASL, pCASL, and [<sup>15</sup>O]H<sub>2</sub>O PET scans using the individual GM masks. Next, these CBF values were compared with each other using a paired  $t$ -test applying a two-tailed significance level of 0.05. A Bland-Altman analysis<sup>35</sup> was performed to investigate the spread and measurement agreement between dual VS-ASL and [<sup>15</sup>O]H<sub>2</sub>O PET. Bias and 95% limits of agreement were calculated as mean difference and as 1.96 × s.d. of difference between paired measurements respectively.

A one-way analysis of variance was performed to compare the tSNRs for the different ASL techniques. To determine the tSNR in GM, both mean ( $\mu$ ) and s.e.m. ( $\sigma/\sqrt{n}$ ) were calculated voxel by voxel over the pairwise subtracted ASL maps before averaging:

$$tSNR = \frac{\mu\sqrt{n}}{\sigma} \quad (4)$$

Since single VS-ASL and AccASL scans cannot be quantified, the comparison for these scans focussed only on the tSNR and the distribution of the signal. In Matlab (R2012b, The MathWorks, Natick, MA, USA), all scans were normalized by dividing each voxel by the average signal intensity in GM. The distribution agreement between the group-averaged normalized scans was visualized in a joint histogram: ASL versus [<sup>15</sup>O]H<sub>2</sub>O-derived CBF. The linear correlation coefficient (Pearson's  $r$ ) was obtained to estimate the degree of correlation between ASL and [<sup>15</sup>O]H<sub>2</sub>O-derived CBF and between ASL and [<sup>15</sup>O]H<sub>2</sub>O-derived aCBV measurements.

### RESULTS

Normalized [<sup>15</sup>O]H<sub>2</sub>O PET and ASL images for both the group average and a single subject are shown in Figure 2. For [<sup>15</sup>O]H<sub>2</sub>O PET the lower effective resolution is noticeable. However, the ASL scans had a decreased FOV in the z-direction (images not shown), while PET covers the entire brain. In AccASL and even more in single VS-ASL an increased signal intensity is visible in the sagittal sinus. Only in the [<sup>15</sup>O]H<sub>2</sub>O-derived aCBV maps the circle of Willis is clearly present.

The  $M0_a$ , measured for CBF quantification, was  $3.8 \times 10^6 \pm 0.27 \times 10^6$  and the arterial blood T<sub>1</sub> was  $1789 \pm 42$  ms for females, which was significantly higher than  $1696 \pm 63$  ms for males ( $P < 0.01$ , unpaired Student's  $t$ -test). The mean GM CBF

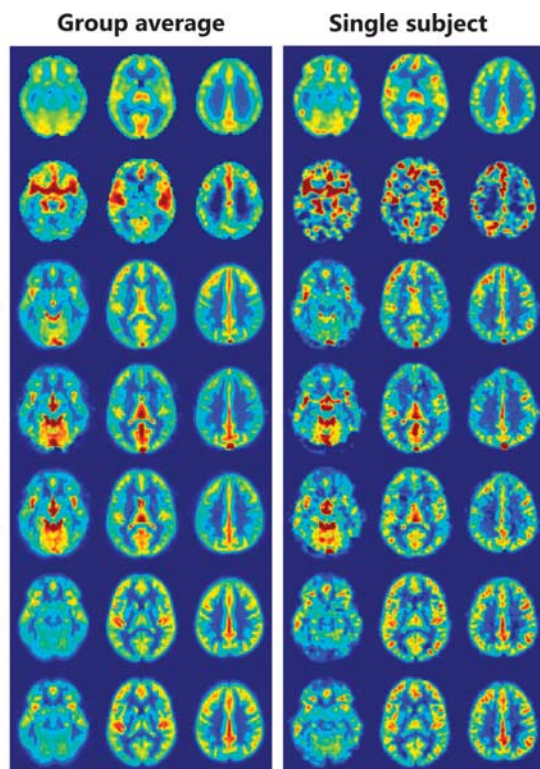


**Figure 2.** Example of three transversal slice of the [<sup>15</sup>O]H<sub>2</sub>O PET and arterial spin labeling maps of both the group average and a single subject. For comparison of the spatial distribution of the signal, all maps were normalized dividing each voxel by the average gray matter value of the corresponding map. AccASL, acceleration-selective arterial spin labeling; aCBV, arterial cerebral blood volume; CBF, cerebral blood flow; pCASL, pseudo-continuous ASL; PET, positron emission tomography; VS-ASL, velocity-selective ASL.

**Table 2.** The average GM CBF (in mL/100 g/min) in the quantifiable ASL and PET scans and the tSNRs of the five different ASL scans, both evaluated at subject level (mean ± s.d.)

	PET CBF	AccASL	Single VS-ASL	Dual VS-ASL	pCASL no crush	pCASL crush
GM CBF	47.1 ± 6.5			46.7 ± 4.1	60.7 ± 10.9	49.2 ± 9.2
tSNR		6.96 ± 1.42	5.04 ± 0.85	3.49 ± 0.50	8.40 ± 1.41	7.05 ± 1.19

Abbreviations: AccASL, acceleration-selective arterial spin labeling; GM CBF, gray matter cerebral blood flow; pCASL, pseudo-continuous ASL; PET, positron emission tomography; tSNRs, temporal signal-to-noise ratios; VS-ASL, velocity-selective ASL.

values for dual VS-ASL, pCASL, and  $[^{15}\text{O}]\text{H}_2\text{O}$  PET are shown in Table 2, together with the GM tSNR of all ASL scans. Analysis of variance indicated a significant difference in tSNR at the  $P < 0.05$  level for the different ASL techniques ( $F(4, 60) = 37.65$ ,  $P = 9.82 \times 10^{-16}$ ). Post hoc comparisons using the Tukey honest significant difference (HSD) test indicated that the mean tSNR of all ASL techniques were significantly different from each other ( $P < 0.05$ ), except for the tSNR of AccASL and noncrushed pCASL ( $P = 0.80$ ). The Bland-Altman plot (Figure 3) showed no bias between the mean GM CBF of dual VS-ASL and  $[^{15}\text{O}]\text{H}_2\text{O}$  PET. On average the GM CBF of dual VS-ASL was only 0.4 mL/100g/min smaller and the paired  $t$ -test did not show a significant difference. Furthermore, regression analysis showed no significant bias ( $P = 0.15$ ). Moreover, the mean GM CBF value of dual VS-ASL was significantly lower than pCASL without vascular crushing ( $P < 0.001$ ). Compared with pCASL with vascular crushing no significant differences were found with the paired  $t$ -test. In Figure 4 the intracranial and GM-normalized group average of the ASL signal versus  $[^{15}\text{O}]\text{H}_2\text{O}$ -derived CBF is plotted voxelwise in a joint histogram. In Table 3 the correlation coefficients between ASL and  $[^{15}\text{O}]\text{H}_2\text{O}$ -derived CBF evaluated at subject level are shown,

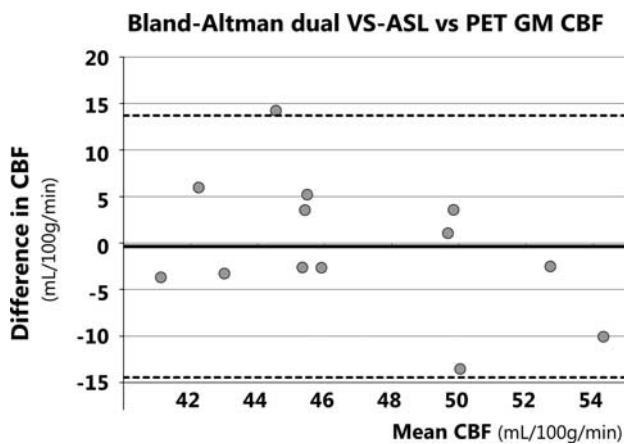


**Figure 3.** Bland-Altman plot of dual VS-ASL and  $[^{15}\text{O}]\text{H}_2\text{O}$  PET CBF in gray matter. The solid line depicts the mean difference between dual VS-ASL and PET CBF over all volunteers, the dashed lines the corresponding 95% confidence intervals. CBF, cerebral blood flow; GM, gray matter; PET, positron emission tomography; VS-ASL, velocity-selective ASL.

with an average range between 0.72 and 0.91 when only including slices above the circle of Willis, between 0.62 and 0.85 for all the intracranial tissues and between 0.13 and 0.39 for the GM tissue only. The correlation coefficients with PET CBF for AccASL, both pCASL scans and to a lesser extent dual VS-ASL were comparable. Only single VS-ASL showed a lower correlation and larger s.d. In Table 3 the correlation coefficients between the various ASL modalities with  $[^{15}\text{O}]\text{H}_2\text{O}$ -derived aCBV are presented as well. For all ASL sequences the correlation coefficients with PET aCBV were lower than PET CBF ( $P < 0.001$ ). The correlation coefficients, intracranial and above the circle of Willis with  $[^{15}\text{O}]\text{H}_2\text{O}$ -derived aCBV of AccASL and both pCASL scans were similar; but both VS-ASL methods showed a lower correlation. The correlation coefficients in GM of all SNS-ASL methods with PET aCBV were significantly lower than pCASL.

## DISCUSSION

In the current study, we compared three SNS-ASL techniques with the gold standard  $[^{15}\text{O}]\text{H}_2\text{O}$  PET and showed pCASL scans, with and without vascular crushing, as a reference for traditional, spatially selective ASL. In addition, the correlation of these ASL methods with aCBV was assessed. To the best of our knowledge this is the first study to extensively compare these SNS-ASL methods with  $[^{15}\text{O}]\text{H}_2\text{O}$  PET. The most important findings of the present study are threefold. First, the GM CBF obtained with dual VS-ASL was similar to  $[^{15}\text{O}]\text{H}_2\text{O}$  PET. Second, the spatial signal distribution of the SNS-ASL methods showed good agreement with that of  $[^{15}\text{O}]\text{H}_2\text{O}$ -derived CBF. Finally, for all SNS-ASL methods the aCBV signal distribution was less present compared with pCASL.

From the three SNS-ASL methods only the CBF of dual VS-ASL can be evaluated quantitatively. The average GM CBF was calculated using the equation proposed by Wu and Wong,<sup>10</sup> with an additional correction factor to account for the two background suppression pulses and a labeling efficiency term, which was estimated by the echo time (TE) of the labeling module and the  $T_2$  of arterial blood, i.e.,  $\exp(-TE_{\text{lab}}/T_{2a})$ . No significant difference was found between the GM CBF obtained using dual VS-ASL and  $[^{15}\text{O}]\text{H}_2\text{O}$  PET, as shown in the Bland-Altman plot (Figure 3). A limitation is that for pCASL and  $[^{15}\text{O}]\text{H}_2\text{O}$  PET a two-compartment model was used, whereas for dual VS-ASL a single-compartment model was used to quantify the CBF. As stated in the ASL consensus paper, the single-compartment model is an oversimplification of the real situation.<sup>3</sup> Therefore, a more comprehensive model, expressed in equation 2, was used to compare the

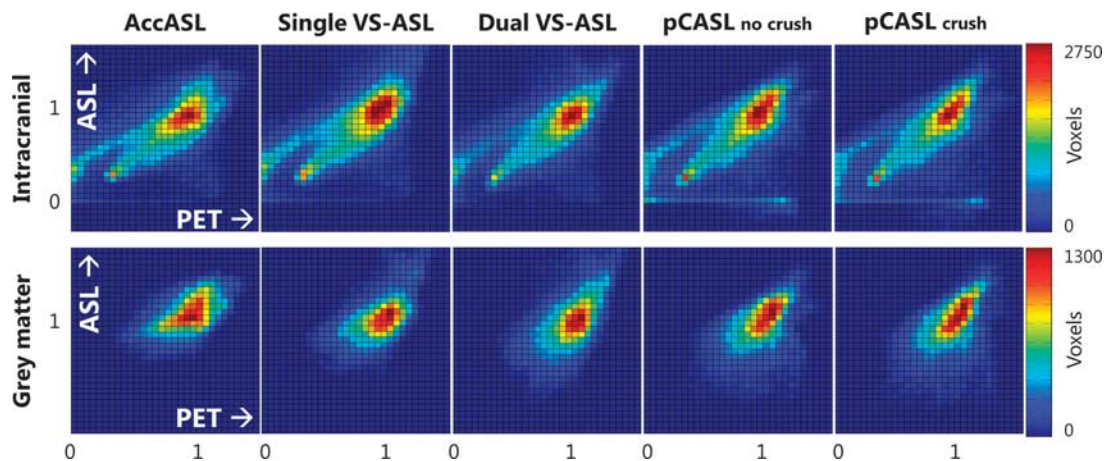


**Figure 4.** Voxelwise joint histograms (34 × 30 bins) of ASL versus  $[^{15}\text{O}]\text{H}_2\text{O}$  PET CBF of intracranial (top) and gray matter (bottom) intensity normalized group-averaged maps. AccASL, acceleration-selective arterial spin labeling; CBF, cerebral blood flow; pCASL, pseudo-continuous ASL; PET, positron emission tomography; VS-ASL, velocity-selective ASL.

**Table 3.** Intracranial (IC), above the CoW, and GM intensity normalized correlation coefficient between ASL and [<sup>15</sup>O]H<sub>2</sub>O PET CBF evaluated at subject level (mean ± s.d.)

	AccASL	Single VS-ASL	Dual VS-ASL	pCASL no crush	pCASL crush
<i>Correlation with PET CBF</i>					
IC	0.85 ± 0.02	0.62 ± 0.08	0.65 ± 0.03	0.84 ± 0.01	0.82 ± 0.02
Above CoW	0.89 ± 0.02	0.72 ± 0.08	0.84 ± 0.02	0.91 ± 0.01	0.91 ± 0.02
GM	0.35 ± 0.06	0.13 ± 0.06	0.14 ± 0.06	0.38 ± 0.05	0.39 ± 0.06
<i>Correlation with PET aCBV</i>					
IC	0.72 ± 0.06	0.54 ± 0.09	0.58 ± 0.06	0.74 ± 0.06	0.73 ± 0.06
Above CoW	0.75 ± 0.06	0.60 ± 0.10	0.70 ± 0.06	0.79 ± 0.06	0.79 ± 0.06
GM	0.15 ± 0.06	0.03 ± 0.06	0.11 ± 0.06	0.28 ± 0.07	0.28 ± 0.07

Abbreviations: aCBV, arterial cerebral blood volume; AccASL, acceleration-selective arterial spin labeling; CBF, cerebral blood flow; CoW, circle of Willis; GM, gray matter; pCASL, pseudo-continuous ASL; PET, positron emission tomography; VS-ASL, velocity-selective ASL.

traditional quantitative ASL data to the gold standard. For dual VS-ASL no validated two-compartment model is available yet, because it is more difficult to estimate the transition moment from the arterial to the tissue compartment because of the large width of the bolus. Another limitation is that a constant, brain average blood-water partition coefficient was assumed in the ASL quantification, although it is known that this is a function of the hematocrit that may vary between subjects. Furthermore, the partition coefficient also varies throughout the brain, since the water content of the tissue is not constant for the different brain regions.<sup>25</sup> Since for [<sup>15</sup>O]H<sub>2</sub>O PET a region-specific volume of distribution was calculated, GM-WM discrepancies might occur between both modalities. Nevertheless, the influence on the quantitative CBF comparison is hypothesized to be limited, since this was only performed in GM.

For single and dual VS-ASL hyperintensities were observed in the posterior flow territory and hypointensities in the anterior flow territory as shown in Figure 2. We think this might be caused by differences in the large vasculature in these regions, like for example the main direction of the vessels is more consistent in the feet-head direction for the posterior than for the anterior circulation.

With VS-ASL it is possible to create label closer to the tissue than with pCASL and therefore it might be considered unnecessary that the PLD for VS-ASL was chosen (slightly) longer than for pCASL. Since the only perfusion signal that is detected in dual VS-ASL is from spins whose velocity was above the  $V_c$  during labeling and below the  $V_c$  during imaging, a certain time between the labeling modules is necessary to let the labeled spins progress through the vascular tree, thereby steadily decreasing their velocity. A too short PLD would therefore lead to too little signal and the PLD in VS-ASL shares, therefore, some resemblance to the labeling duration of pCASL and the Quantitative imaging of perfusion using a single subtraction (QUIPSS) time of a pulsed arterial spin labeling (PASL) experiment. Therefore, the PLD of VS-ASL was chosen similar to the labeling duration and PLD of the pCASL experiments. For comparison reasons, the PLD of single VS-ASL and AccASL were kept equal to the PLD of dual VS-ASL.

The use of a second labeling module in dual VS-ASL allows quantifications of CBF, but will eliminate part of the arterial signal as well and thus decrease the amount of detected signal. This will not influence the quantitative estimation of the CBF, since it is corrected for in the quantification equation, but it will decrease the tSNR. This decrease in tSNR adds to the already lower tSNR of SNS-ASL because of the use of saturation instead of inversion for labeling.

Although the pCASL data in this study were included for reference purposes only, it was noticed that the calculated mean GM CBF values in this subgroup of subjects was  $9.8 \pm 4.4$  mL/100 g/min higher than reported by Heijtel *et al.*<sup>12</sup> The main reason for

this difference was that some volunteers who were included in the current analysis, were not included in the previous reported analysis and vice versa. When performing the analysis with only the subjects who were included in both studies ( $n=10$ ), the difference for the noncrushed pCASL CBF is then 5.1 mL/100 g/min. The remaining difference can be explained by the slightly different approaches to create GM masks, such as registration to MNI instead of the use of a group-specific atlas and accompanying differences in thresholds.

The comparison of AccASL and single VS-ASL with [<sup>15</sup>O]H<sub>2</sub>O-derived CBF solely focussed on the tSNR and the spatial distribution of the signal by normalized maps, joint histograms, and the calculated correlation coefficients, as these ASL techniques cannot be quantified. When both modalities would have had the same signal distribution, the joint histograms would have shown a straight line as evidence of good agreement. As both the ASL and [<sup>15</sup>O]H<sub>2</sub>O PET data were normalized to the average signal intensity of the GM, the slope of the line has no specific meaning. In Figure 4 it can clearly be seen that the ASL methods showed a good intracranial correlation with PET CBF. White matter is represented in the left bottom corner, because the perfusion of WM is lower than that of GM. For [<sup>15</sup>O]H<sub>2</sub>O PET a region-specific volume of distribution was calculated for the blood-water partition coefficient. However, the correlation coefficients were calculated using the ASL data without regional correction for the partition coefficient, which will induce GM-WM discrepancies between both modalities and might have led to lower correlation values. Some of the other discrepancies can be explained by the EPI readout, as can be seen in Figure 2: it has been shown previously that the EPI readout is prone to signal loss in the prefrontal brain area.<sup>36</sup> Furthermore, the timing of background suppression pulses was rather aggressive, which could have led to some signal loss in the lowest slices.

Focussing at the correlation coefficients as presented in Table 3, it is clear that compared with all other ASL techniques single VS-ASL showed the lowest correlation with [<sup>15</sup>O]H<sub>2</sub>O-derived CBF. This weaker correlation could be explained by the presence of venous signal, of which the high signal intensity in the sagittal sinus is a good example, which is less obvious in AccASL and even absent in the other ASL sequences. Furthermore, it is known that single VS-ASL, and again to a lesser extent for AccASL, has higher signal in CSF regions, owing to the combination of a relatively high amount of diffusion and flow in CSF. The diffusion weighting of the labeling module is strong enough to cause diffusion-related attenuation in CSF and thereby contamination of the CBF maps.<sup>6</sup> To incorporate this contamination into our validation analysis, it was decided to compare signal distribution over the entire brain between ASL and PET (i.e., including ventricles and sagittal sinus). In addition, the signal distribution of only the GM tissue was analyzed separately. Single VS-ASL showed less signal than

AccASL, which could be surprising since the labeling block of VS-ASL also exhibits a nonzero second moment, thereby also providing acceleration-insensitive labeling. One could speculate that the combined velocity- and acceleration-sensitive signal would lead to more signal, however, this was not observed. This might be partially explained by the fact that the first and second moment of the VS-labeling module have an opposite sign and will therefore not add constructively. Furthermore, because of the difference in gradient amplitude for VS-ASL compared with AccASL, the acceleration cutoff is higher, which could mean that the labeling is in a different region and probably further away from the capillaries.

For both single VS-ASL and AccASL, it has been postulated that they would be more weighted toward CBV than CBF, since all blood above a certain velocity or acceleration is labeled.<sup>7</sup> To investigate this hypothesis, weighting toward aCBV was studied. By examining the intracranial and GM correlation coefficients of ASL with [<sup>15</sup>O]H<sub>2</sub>O-derived aCBV. The highest intracranial correlations with PET aCBV were observed for pCASL and AccASL, closely followed by dual VS-ASL. Only the intracranial correlation coefficient of single VS-ASL with PET aCBV differed from the other sequences, being ~20% lower than the traditional ASL methods. The GM correlations coefficients with PET aCBV of the SNS-ASL methods were lower than pCASL. The GM correlations with PET aCBV of dual VS-ASL showed the most resemblance to pCASL, followed by AccASL, and single VS-ASL again had the lowest correlation. However, all ASL methods showed lower correlation coefficients with PET aCBV than with PET CBF. aCBV maps mainly show besides a normal GM/WM contrast, large vessels and the signal is only arterial, whereas the single VS-ASL and AccASL are thought to create label closer to the tissue because of the relatively long PLD and the images also include a venous component.<sup>7,9</sup> In summary, the present results show that single VS-ASL and AccASL have much lower weighting toward aCBV compared with pCASL. Unfortunately, these findings cannot answer the question whether those techniques are more weighted toward total CBV and this remains to be answered.

In the present study, the [<sup>15</sup>O]H<sub>2</sub>O-derived aCBV were used only for comparison of the relative signal distributions and not for quantitative purposes. This approach was followed because of uncertainties in quantitative accuracy of aCBV as measured by [<sup>15</sup>O]H<sub>2</sub>O PET. One problem is the potential confounding effect of dispersion in the arterial line. When the dispersion is not estimated correctly because of artefacts in the image reconstruction, aCBV will become less accurate and could especially show a global bias.<sup>37</sup> Visual inspection of the individual aCBV maps was performed to identify any clear errors, which were not observed. Positron emission tomography would be able to provide more accurate CBV measurements by means of [<sup>15</sup>O]-labeled carbon monoxide (C<sup>15</sup>O).<sup>34</sup>

The study protocol could have been improved by acquiring the PET and ASL scans on the same day or even at the same time, thereby minimizing the effects of the physiologic fluctuations in the perfusion.<sup>38</sup> Unfortunately, this was logistically impossible with the imaging centers at two different locations, since at the time of the study no combined PET/MRI system was available in either of the two centers. Nevertheless, it should be noted that it was verified that both pCASL and VS-ASL show similar variations over time, with changes in the order of 10% or less over a six-month period.<sup>39</sup>

In future work, a comparison of the results from SNS-ASL methods with images that are (totally) CBV weighted should be made, to better understand in the weighting of the different ASL methods. Furthermore, the current recommended clinical application for SNS-ASL is in subjects with slow or collateral flow. Therefore, a comparison between conventional and SNS-ASL methods and [<sup>15</sup>O]H<sub>2</sub>O or [<sup>15</sup>O]CO PET in patients with large-vessel disease could give more insight into the preferred perfusion

measurement technique for such pathologies with delayed arrival times.

In conclusion, dual VS-ASL provides a similar quantitative CBF, and qualitatively all SNS-ASL methods provide similar CBF maps as compared with [<sup>15</sup>O]H<sub>2</sub>O PET. From the SNS-ASL methods, AccASL was most similar to PET CBF, showing only a 2% lower intracranial correlation coefficient compared with pCASL. This opens up the possibility of exploring the clinical applications and validations of SNS-ASL with dual VS-ASL as a quantitative technique and AccASL for qualitative purposes.

## DISCLOSURE/CONFLICT OF INTEREST

The authors declare no conflict of interest.

## REFERENCES

- 1 Detre JA, Leigh JS, Williams DS, Koretsky AP. Perfusion imaging. *Magn Reson Med* 1992; **23**: 37–45.
- 2 Alsop DC, Detre JA. Reduced transit-time sensitivity in noninvasive magnetic resonance imaging of human cerebral blood flow. *J Cereb Blood Flow Metab* 1996; **16**: 1236–1249.
- 3 Alsop DC, Detre JA, Golay X, Gunther M, Hendrikse J, Hernandez-Garcia L et al. Recommended implementation of arterial spin-labeled perfusion MRI for clinical applications: a consensus of the ISMRM perfusion study group and the European consortium for ASL in dementia. *Magn Reson Med* 2015; **73**: 102–116.
- 4 Norris DG, Schwarzbauer C. Velocity selective radiofrequency pulse trains. *J Magn Reson Imaging* 1999; **137**: 231–236.
- 5 Duhamel G, de Bazelaire C, Alsop DC. Evaluation of systematic quantification errors in velocity-selective arterial spin labeling of the brain. *Magn Reson Med* 2003; **50**: 145–153.
- 6 Wong EC, Cronin M, Wu WC, Inglis B, Frank LR, Liu TT. Velocity-selective arterial spin labeling. *Magn Reson Med* 2006; **55**: 1334–1341.
- 7 Schmid S, Ghariq E, Teeuwisse WM, Webb AG, van Osch MJP. Acceleration-selective arterial spin labeling. *Magn Reson Med* 2014; **71**: 191–199.
- 8 Qiu D, Straka M, Zun Z, Bammer R, Moseley ME, Zaharchuk G. CBF measurements using multidelay pseudocontinuous and velocity-selective arterial spin labeling in patients with long arterial transit delays: comparison with xenon CT CBF. *J Magn Reson Imaging* 2012; **36**: 110–119.
- 9 Guo J, Wong EC. *Comparison of transit delay sensitivity between pseudo-continuous ASL, pulsed ASL and velocity-selective ASL*. Milan, Italy: Proc Intl Soc Mag Reson Med, 2014.
- 10 Wu WC, Wong EC. Feasibility of velocity selective arterial spin labeling in functional MRI. *J Cereb Blood Flow Metab* 2007; **27**: 831–838.
- 11 Bokkers RPH, Bremmer JP, van Berckel BNM, Lammertsma AA, Hendrikse J, Pluim JPW et al. Arterial spin labeling perfusion MRI at multiple delay times: a correlative study with H215O positron emission tomography in patients with symptomatic carotid artery occlusion. *J Cereb Blood Flow Metab* 2009; **30**: 222–229.
- 12 Heijtel DF, Mutsaerts HJ, Bakker E, Schober P, Stevens MF, Petersen ET et al. Accuracy and precision of pseudo-continuous arterial spin labeling perfusion during baseline and hypercapnia: a head-to-head comparison with <sup>15</sup>O H<sub>2</sub>O positron emission tomography. *Neuroimage* 2014; **92**: 182–192.
- 13 Priest AN, Graves MJ, Lomas DJ. *Acceleration dependent vascular anatomy for non-contrast-enhanced MRA (ADVANCE-MRA)*. Montreal, Canada: Proc Intl Soc Mag Reson Med, 2011.
- 14 Xu G, Rowley HA, Wu G, Alsop DC, Shankaranarayanan A, Dowling M et al. Reliability and precision of pseudo-continuous arterial spin labeling perfusion MRI on 3.0T and comparison with 15O-water PET in elderly subjects at risk for Alzheimer's disease. *NMR Biomed* 2010; **23**: 286–293.
- 15 Ye FQ, Frank JA, Weinberger DR, McLaughlin AC. Noise reduction in 3D perfusion imaging by attenuating the static signal in arterial spin tagging (ASSIST). *Magn Reson Med* 2000; **44**: 92–100.
- 16 Garcia DM, Duhamel G, Alsop DC. Efficiency of inversion pulses for background suppressed arterial spin labeling. *Magn Reson Med* 2005; **54**: 366–372.
- 17 St Lawrence KS, Frank JA, Bandettini PA, Ye FQ. Noise reduction in multi-slice arterial spin tagging imaging. *Magn Reson Med* 2005; **53**: 735–738.
- 18 Dai W, Garcia D, de Bazelaire C, Alsop D. Continuous flow-driven inversion for arterial spin labeling using pulsed radio frequency and gradient fields. *Magn Reson Med* 2008; **60**: 1488–1497.
- 19 Teeuwisse WM, Schmid S, Helle M, van Osch MJP. *2-shim or not 2-shim, that is a question in pseudo continuous arterial spin labeling*. Milan, Italy: Proc Intl Soc Mag Reson Med, 2014.

- 20 Varela M, Hajnal JV, Petersen ET, Golay X, Merchant N, Larkman DJ. A method for rapid in vivo measurement of blood T1. *NMR Biomed* 2011; **24**: 80–88.
- 21 Smith SM, Jenkinson M, Woolrich MW, Beckmann CF, Behrens TEJ, Johansen-Berg H *et al*. Advances in functional and structural MR image analysis and implementation as FSL. *NeuroImage* 2004; **23**: 208–219.
- 22 Woolrich WM, Jbabdi S, Patenaude B, Chappell M, Makni S, Behrens T *et al*. Bayesian analysis of neuroimaging data in FSL. *Neuroimage* 2009; **45**: 173–186.
- 23 Jenkinson M, Bannister P, Brady M, Smith S. Improved optimisation for the robust and accurate linear registration and motion correction of brain images. *Neuroimage* 2002; **17**: 825–841.
- 24 Teeuwisse WM, Nederveen AJ, Ghariq E, Heijtel DF, Osch MJV. *Comparison of spin dynamics in pseudo-continuous and velocity-selective arterial spin labeling with and without vascular crushing*. Montreal, Canada: Proc Intl Soc Mag Reson Med, 2011.
- 25 Herscovitch P, Raichle ME. What is the correct value for the brain–blood partition coefficient for water? *J Cereb Blood Flow Metab* 1985; **5**: 65–69.
- 26 Chen JJ, Pike GB. Human whole blood T2 relaxometry at 3 Tesla. *Magn Reson Med* 2009; **61**: 249–254.
- 27 Liu P, Uh J, Lu H. Determination of spin compartment in arterial spin labeling MRI. *Magn Reson Med* 2011; **65**: 120–127.
- 28 Lu H, Nagae-Poetscher LM, Golay X, Lin D, Pomper M, van Zijl PC. Routine clinical brain MRI sequences for use at 3.0 Tesla. *J Magn Reson Imaging* 2005; **22**: 13–22.
- 29 Wu WC, Fernandez-Seara M, Detre JA, Wehrli FW, Wang J. A theoretical and experimental investigation of the tagging efficiency of pseudocontinuous arterial spin labeling. *Magn Reson Med* 2007; **58**: 1020–1027.
- 30 Aslan S, Xu F, Wang PL, Uh J, Yezhuvath US, van Osch MJV *et al*. Estimation of labeling efficiency in pseudocontinuous arterial spin labeling. *Magn Reson Med* 2010; **63**: 765–771.
- 31 Ye FQ, Mattay VS, Jezzard P, Frank JA, Weinberger DR, McLaughlin AC. Correction for vascular artifacts in cerebral blood flow values measured by using arterial spin tagging techniques. *Magn Reson Med* 1997; **37**: 226–235.
- 32 Boellaard R, van Lingen A, van Balen SCM, Hoving BG, Lammertsma AA. Characteristics of a new fully programmable blood sampling device for monitoring blood radioactivity during PET. *Eur J Nucl Med* 2001; **28**: 81–89.
- 33 Boellaard R, Knaapen P, Rijbroek A, Luurtsema GJJ, Lammertsma AA. Evaluation of basis function and linear least squares methods for generating parametric blood flow images using <sup>15</sup>O-water and positron emission tomography. *Mol Imaging Biol* 2005; **7**: 273–285.
- 34 Bremmer JP, Berckel BNM, Persoon S, Kappelle LJ, Lammertsma AA, Kloet R *et al*. Day-to-day test–retest variability of CBF, CMRO<sub>2</sub>, and OEF measurements using dynamic <sup>15</sup>O PET studies. *Mol Imaging Biol* 2011; **13**: 759–768.
- 35 Bland JM, Altman DG. Statistical methods for assessing agreement between two methods of clinical measurements. *Lancet* 1986; **1**: 307–310.
- 36 Vidorreta M, Wang Z, Rodriguez I, Pastor MA, Detre JA, Fernandez-Seara MA. Comparison of 2D and 3D single-shot ASL perfusion fMRI sequences. *Neuroimage* 2013; **66**: 662–671.
- 37 Lammertsma AA, Jones T. Correction for the presence of intravascular oxygen-15 in the steady-state technique for measuring regional oxygen extraction ratio in the brain: 1. Description of the method. *J Cereb Blood Flow Metab* 1983; **3**: 416–424.
- 38 Zhang K, Herzog H, Mauler J, Filss C, Okell TW, Kops ER *et al*. Comparison of cerebral blood flow acquired by simultaneous <sup>15</sup>O water positron emission tomography and arterial spin labeling magnetic resonance imaging. *J Cereb Blood Flow Metab* 2014; **34**: 1373–1380.
- 39 Zun Z, Qiu D, Rosenberg J, Zaharchuk G. *Longitudinal study of cerebral blood flow measurements in normals using pseudocontinuous and velocity-selective arterial spin labeling*. Salt Lake City, UT: Proc Intl Soc Mag Reson Med, 2013.